Integrated Optics at 10.6-μm Wavelength

WILLIAM S. C. CHANG, SENIOR MEMBER, IEEE

(*Invited Paper*)

Abstract—**While the major objective of integrated optics at the visible-light and near-infrared wavelength is to provide thin-film components to obtain switching, modulation, source, detection, etc., for fiber-optics communication, the immediate objective of integrated optics at the 10.6-μm wavelength is to improve the operational characteristics of conventional bulk components via guided-wave technology. This paper will discuss the properties of the waveguides, the modulators, the passive components, and the waveguide laser that have been made to date. The most significant advancement is probably guided-wave modulation. Both the analysis and the initial experimental measurements indicate that π-phase or 100-percent amplitude UHF–VHF modulation could be obtained with only a few hundred watts of modulation drive power. Microwave modulation has also been experimentally demonstrated. Naturally, this is only an interim report. Many exciting developments will be obtained in the future.**

I. INTRODUCTION

THERE are no fibers that can be used effectively to transmit optical signals over kilometers of distance at the far infrared. On the other hand, conventional active components such as electrooptical modulators function very poorly at the long wavelength; the need exists for two to three orders of magnitude improvement in the efficiency of these active devices. Thus the primary objective of the present integrated-optics research at the 10.6-μm wavelength is to utilize the guided-wave technique to achieve more efficient and wide-band modulation, switching, and multiplexing of CO_2-laser radiation. These components may be used to perform a single system function such as modulation. Several integrated optical components may also be used together as a subsystem in a given communications system. Their ultimate success will be determined by their operating characteristics as compared to their counterparts presently being developed in the bulk form. For example, tunable wide-band (>1-GHz) CO_2 waveguide laser sources are being developed at NASA, Hughes, and United Aircraft Laboratories [1]–[2]. One could also compare the modulation that can be achieved through an intracavity coupling modulator [3]–[5] with those achievable with the thin-film waveguide techniques discussed later in this paper. Thin-film HgCdTe–CdTe heterodyne detectors are currently being investigated at Lincoln Laboratories [6]. A by-product of the research is the demonstration of integrated optical components without the extreme accuracy required for the fabrication processes at the shorter visible-light wavelength.

This paper will discuss the various waveguides that have been reported, the characteristics of the devices that have been fabricated, and the extent to which these may be predicted from theoretical calculations.

II. THIN-FILM WAVEGUIDES

Very few materials are transparent at the 10.6-μm wavelength. Almost any material that contains light elements such as oxygen, hydrogen, or nitrogen will absorb at the far infrared. Consequently, low-loss optical materials at the 10.6-μm wavelength are limited to rock salts such as NaCl, the semiconductor element Ge, III–V semiconductors such as GaAs, II–VI semiconductors such as CdTe, and the infrared Kodak IRTRAN and Texas Instruments glasses [7], [8].

In principle, any high-index material can be sputtered or deposited onto a lower index substrate to form a waveguide. Ge on IRTRAN II was reported as a waveguide in 1971 [9]. But a passive waveguide is useful only to interconnect active components; it cannot be used as a modulator or a switch. Hence recent interests have been concentrated on III–V and II–VI semiconductor thin-film waveguides.

Waveguiding in GaAs epitaxial film grown by the vapor phase-epitaxy technique on an n^+GaAs substrate was first reported by Hall *et al.* at the 1.15-μm wavelength [10]. Subsequently, Cheo *et al.* reported properties of GaAs epitaxial thin-film waveguide grown on an n^+GaAs substrate at 10.6-μm [11]. Finn *et al.* reported properties of GaAs epitaxial thin-film waveguide on an GaAsP substrate in 1973 [12]. Recently, McFee reported GaAs waveguide grown on an GaAlAs substrate [13].

A. GaAs/n^+GaAs Waveguide

Whenever free carriers are present in GaAs, they will affect both the refractive index and the absorption coefficient of the material. The absorption coefficient of GaAs at the 10.6-μm wavelength can be written approximately as

$$\alpha = 8 \cdot 10^{-17} N \text{ cm}^{-1} \quad (1)$$

when N is the free-carrier concentration in carriers per cubic centimeters.

Manuscript received April 8, 1974; revised July 25, 1974. This work was supported in part by the National Science Foundation under Grant GK 31854, in part by ARPA/AFCRL Contract F 19628-72-C-0324 to the Monsanto Company–Washington University, and in part by a British Science Research Council Senior Visiting Fellowship.

The author was on sabbatical leave at University College, London, England. He is with the Department of Electrical Engineering and the Laboratory for Applied Electronics Sciences, Washington University, St. Louis, Mo. 63130.

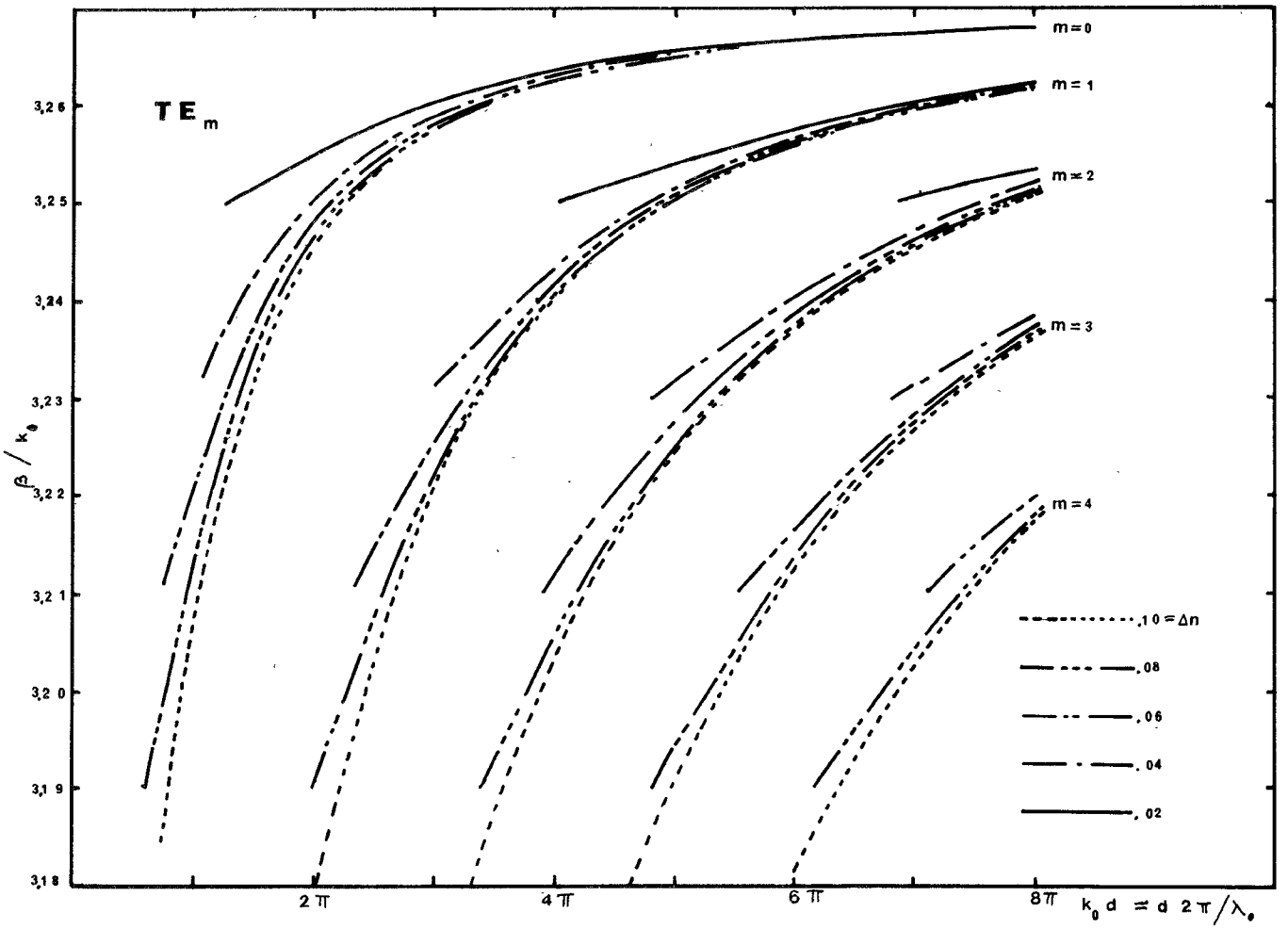

Fig. 1. Propagation wavenumber of TE_m modes in GaAs epitaxial waveguides.

The refractive index n is affected both by absorption through the extinction coefficient

$$K_e = \alpha\lambda/4\pi \tag{2}$$

and by the electric susceptibility of the free carriers

$$\chi_e = Ne^2/\omega m^* \tag{3}$$

where $\omega = 2\pi f$ is the optical angular frequency; e is the electric charge of an electron; m^* is the effective mass; and λ is the free-space wavelength:

$$n^2 = \epsilon_\infty - 4\pi\chi_e + K_e^2.$$

For the 10.6-μm wavelength

$$n \cong (10.7 - 1.53 \cdot 10^{-18}N)^{1/2}. \tag{4}$$

From the preceding relationship between n and N, the waveguiding properties of the intrinsic GaAs film ($N_f < 10^{15}$) on an n^+ substrate having a given carrier concentration N_s can be calculated by the usual equations for TE and TM modes [14], [15]. Figs. 1 and 2 show the propagation wavenumber β of the TE and TM modes in epitaxial waveguide for various values of Δn and thickness d. Here, Δn is the difference of the refractive index between the film (n_f) and the substrate (n_s). Clearly, a larger N_s will yield both a larger Δn and a shorter evanescent tail of the electric field in the substrate; but a larger N_s will also yield a larger absorption coefficient α. Figs. 3 and 4 show the calculated attenuation rate of GaAs/n^+GaAs waveguides as a function of the substrate carrier concentration. Fig. 5 shows the experimentally measured attenuation rate of the TE_0 mode as a function of the film thickness for a variety of the substrates. Clearly, the GaAs/n^+GaAs waveguides will have low loss for thick films on high carrier-concentration substrates and high loss for thin films.

In practice, large-area (with sample length up to 6 cm) and good-quality film (with surface irregularity less than 0.1 μm) has been grown on the (100) surface of n^+GaAs by the vapor phase-epitaxy technique. For undoped GaAs films, the chloride-vapor phase-epitaxy technique gives a better carrier concentration ($N_f \cong 10^{12}$). The vapor phase-epitaxy technique using the Group-V hydride feed system gives N_f in the order of 10^{13}.

B. GaAs/GaAsP and GaAs/GaAlAs Waveguides

In order to provide low-attenuation waveguides at a film thickness not very far from the cutoff of the lowest order modes, e.g., less than 10 μm thick, one must reduce N_s but maintain the Δn. This can be achieved if the substrate is made from either $GaAs_{1-x}P_x$ or $Ga_{1-y}Al_yAs$. The

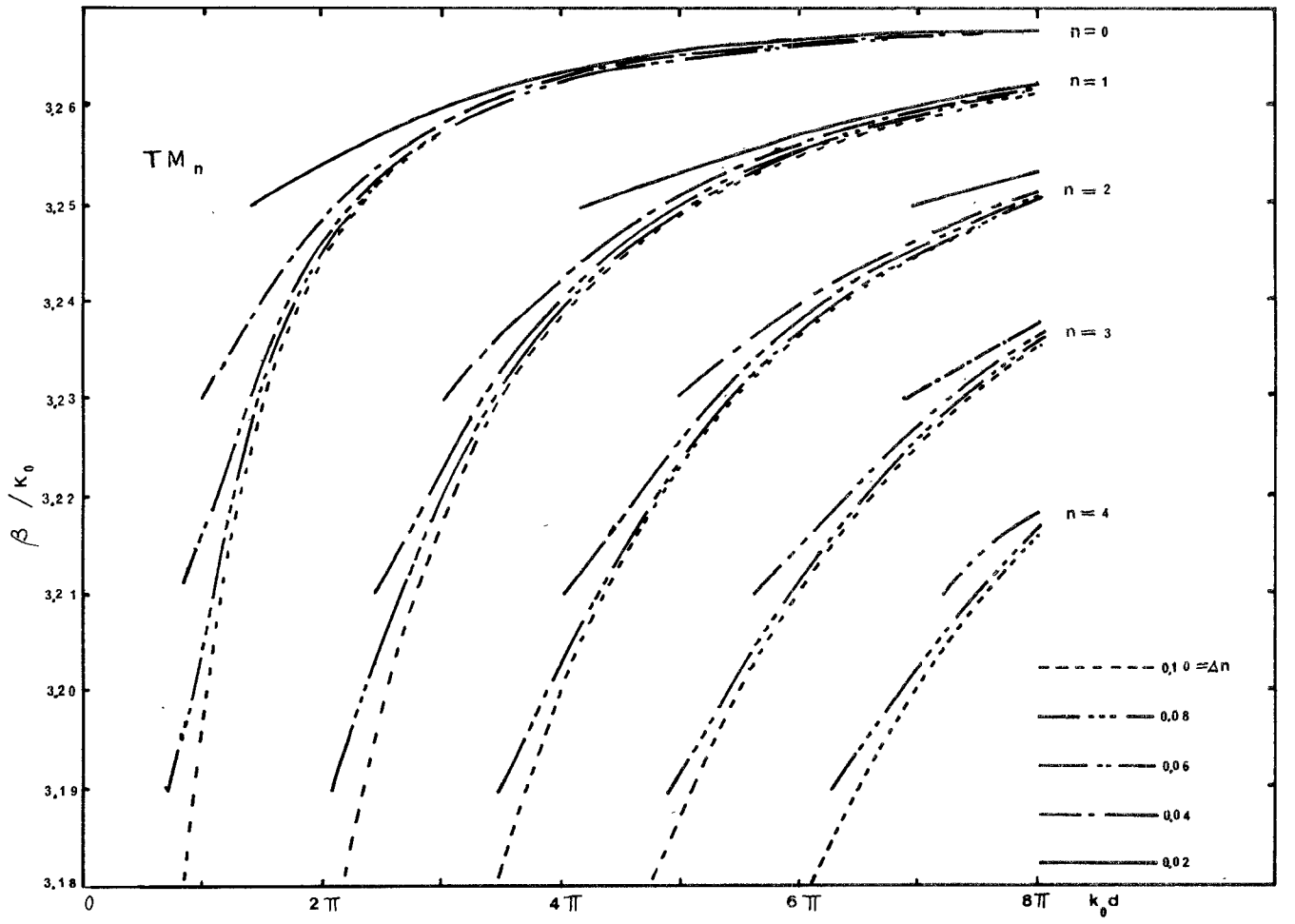

Fig. 2. Propagation wavenumber of TM_n modes in GaAs epitaxial waveguides.

refractive index of $GaAs_{1-x}P_x$ and $Ga_{1-y}Al_yAs$ is lower than the refractive index of GaAs by $\Delta n = 0.4x$ and $\Delta n = 0.43y$.

In principle, the GaAs/GaAsP and the GaAs/GaAlAs waveguides should have identical characteristics as long as they have the same Δn value. For a given Δn, the β values of the various modes were given in Figs. 1 and 2. But in practice GaAsP is grown by the vapor phase-epitaxy technique from a base sample of GaAs using the Group-V hydride feed system and the HCl transport of the gallium. GaAlAs is grown by the liquid phase-epitaxy technique. The quality of the film, the carrier concentration, the control of the film uniformity and thickness, and the sample size that can be obtained by the two techniques are quite different. So far, the GaAs/GaAsP waveguide up to 5 cm in length has been reported by the Monsanto–Washington University group [12] and a GaAs/GaAlAs waveguide 1–2 cm in size has been reported by Bell Laboratories [13]. Large-area GaAlAs epitaxial layer (without the GaAs waveguiding film), has been reported by Hughes Research Laboratory [16]. Past experience at the Monsanto Company seems to indicate that low carrier concentrations, fine thickness and composition control (including the possibility of a graded-index waveguide), and large sample size (5 cm or larger) may be achieved more easily by the vapor phase-epitaxy technique. But unlike the GaAs film with $N_f \cong 10^{12}$ grown by the usual chloride-vapor phase-epitaxy technique, the carrier concentration N_f is slightly higher for the hydride-vapor phase-epitaxial film $N \cong 10^{13}$. The carrier concentrations that can be obtained in the liquid phase-epitaxy technique was reported by McFee *et al.* to be approximately 10^{16}. In short, no definitive conclusions can yet be drawn about the relative merits of the two material-growth processes for the fabrication of far-infrared waveguides.

Experimentally measured attenuation rate at 1–2 dB/cm for the TE_0 mode has been achieved both in GaAs/GaAsP and in GaAs/GaAlAs waveguides [6], [7]. Note the experimental data of the GaAs/GaAsP waveguide shown in Fig. 5. The data clearly demonstrated the advantage of GaAs/GaAsP and GaAs/GaAlAs waveguides at small thicknesses. However, attenuation in intrinsic bulk GaAs has been measured to be 0.05 dB/cm [17]. The residual discrepancy in the attenuation rate between bulk GaAs and thin-film GaAs is not well understood. As it is in the GaAs/n^+GaAs waveguides, free-carrier concentration in the GaAsP or in the GaAlAs substrate will cause waveguide attenuation Fig. 6 shows the calculated attenuation rate as a function of film thickness for various Δn values where N_s is 10^{16}. Clearly, the waveguide attenuation caused

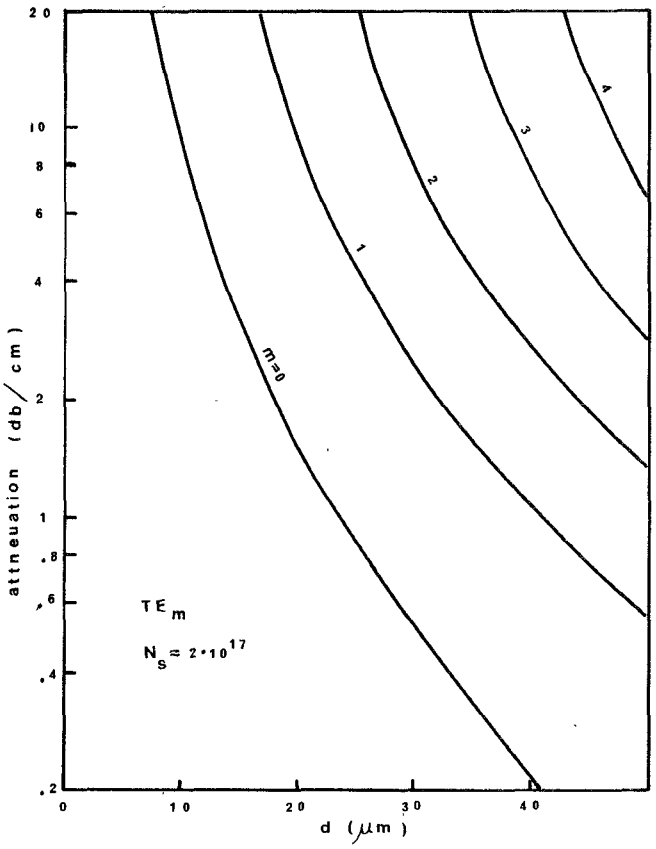

Fig. 3. Attenuation rate of GaAs/n+GaAs waveguides.

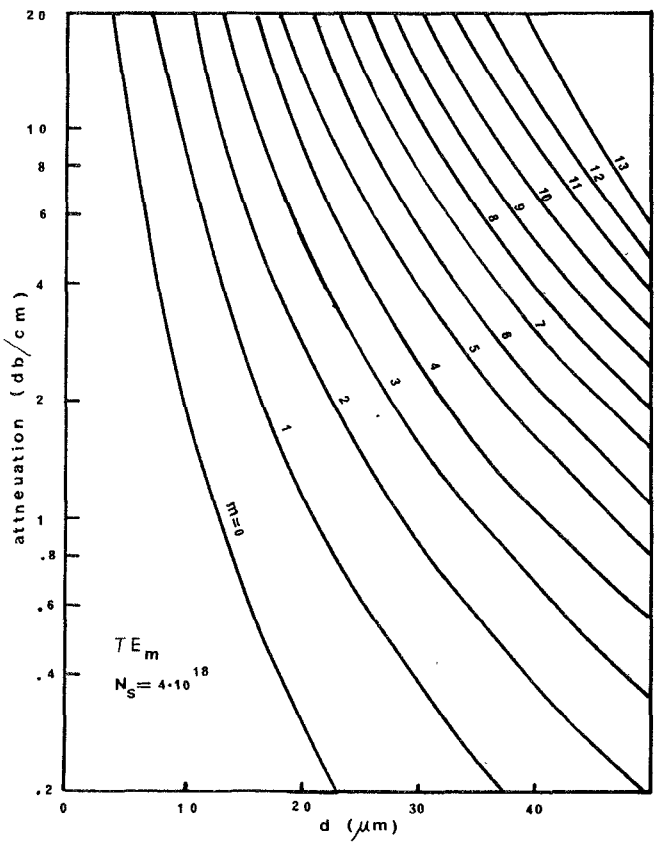

Fig. 4. Attenuation rate of GaAs/n+GaAs waveguides.

by substrate free-carrier absorption will be less than 1 dB/cm for $N_s \leq 10^{16}$ unless the mode is very close to cutoff.

C. Waveguides in Other Semiconductors

Since II–VI semiconductors are transparent at the 10.6-μm wavelength and have a high electrooptical coefficient, they are good materials for making active waveguides. Diffused waveguides of (Zn,Cd)Se, (Zn,Cd)S, Zn(S,Se), and Cd(S,Se) were reported for propagation at the 0.6328-μm wavelength [18]. Waveguides of PbTe grown epitaxially on BaF_2 were reported by Weber and Yeung for 6.5-μm wavelength propagation [19].

Very recently, low-loss waveguides in CdTe produced by high-energy proton bombardment were reported by Spears *et al.* [20]. They start with a CdTe substrate with carrier concentrations in the 10^{17}–10^{18}-carriers/cm^3 range. Proton bombardment removed most of the free carriers and produced a waveguide 30–50 μm thick. Waveguide attenuations were measured experimentally to be in the range of 1 cm^{-1} (i.e., 4 dB/cm).

D. Two-Dimensional Waveguides

A two-dimensional waveguide was chemically etched from the uniform thin-film waveguide of GaAs/n^+GaAs [21]. An SiO_2 mask was first made by the usual photolitography technique on a GaAs/n^+GaAs sample 5 × 2 × 0.025 cm in size with a 25-μm-thick GaAs film. Following that the GaAs is etched about 25 μm deep by H_2SO_4:H_2O_2:H_2O (3:1:1) at 45°C. The SiO_2 mask is finally removed by HF. The edge irregularities caused by the chemical etching process are much less than 1 μm. The waveguides have tapered transitions at both ends so that prism couplers could be used to excite and to couple out from the one-dimensional waveguide modes in the usual manner; the tapered transition then converts the one-dimensional mode into a two-dimensional mode. By adjusting the angle of incidence of the laser beam with respect to the film surface one selects the order p of the $E_{pq}{}^y$ and $E_{pq}{}^x$ modes for excitation. By adjusting the orientation of the prism with respect to the axis of the waveguide, one selects the order q. At large waveguide width such as 50 μm it is difficult to excite just one order of q.

No measurable increase in attenuation was observed for the 50-μm-wide two-dimensional waveguide modes, $E_{1q}{}^y$ and $E_{2q}{}^y$ (at low orders of q), as compared to the TE_0 and TE_1 one-dimensional waveguide modes. When a 25-μm-wide two-dimensional waveguide is measured, the $E_{1q}{}^y$ modes have 1 dB/cm more attenuation than the TE_0 modes; the $E_{2q}{}^y$ modes have 6 dB/cm more attenuation than the TE_1 modes.

III. MODULATION

A. Electrooptical Phase Modulation

When an electric field is applied to the electrooptical thin-film waveguide, it will cause a change in phase $\Delta\phi$ of the specific mode propagation in the waveguide. Phase modulation was achieved in this manner by Cheo, as

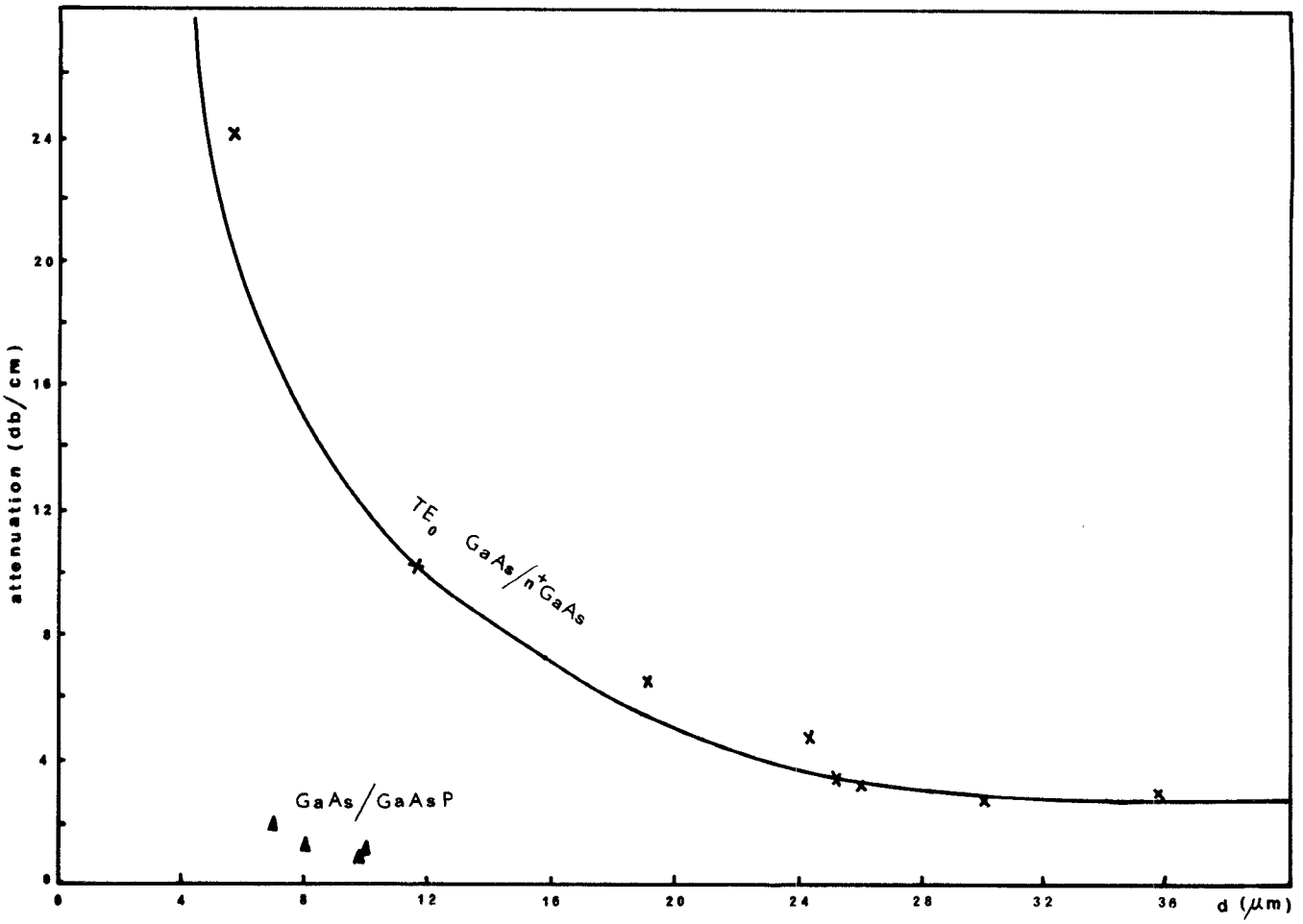

Fig. 5. Measured attenuation rate of the TE_0 mode in GaAs/n$^+$GaAs and in GaAs/GaAsP waveguides.

shown in Fig. 7, in a GaAs/n^+GaAs waveguide [22]. At a film thickness of $d = 17.3$ μm he obtained $\Delta\phi \cong \frac{1}{2}$ radiant at $V = 80$ V of modulation voltage over an electrode $l = 1$ cm long.

If one approximates the lowest order mode in a thick waveguide by a plane wave propagating in the thin film with constant electric-field strength within the film and zero electric field outside, then

$$\Delta\phi \cong k_0 l \Delta n \cong k_0 (n_f^3 r_{41}/2) lV/d. \tag{5}$$

Here the applied modulation electric field is along the 100 direction perpendicular to the film. The n^+ substrate is assumed to have much lower electrical resistivity than the film. Consequently, the modulation electric-field strength in the film is $E_{\text{mod}} \simeq V/d$. The guided wave is assumed to be polarized along the film so that Δn is $n_f^3 r_{41} E_{\text{mod}}/2$. r_{41} is the electrooptical coefficient of GaAs ($r_{41} \simeq 1.2 \times 10^{-12}$ m/V). k_0 is the free-space propagating wavenumber, $k_0 = 2\pi/\lambda$, where $\lambda = 10.6$ μm. Based upon this approximate result we see that the voltage needed for π radiant phase modulation is

$$V_\pi = \frac{\lambda}{n_f^3 r_{41}} \cdot \frac{d}{l}. \tag{6}$$

For Cheo's modulator we can estimate that $V_\pi \cong 500$ V for $l = 1$ cm or $V_\pi \simeq 100$ V for $l = 5$ cm. In order to limit the dissipation of modulation power, Cheo made the top electrode into a reserve-biased Schottky barrier.

It is interesting to note that avalanche breakdown in GaAs would limit the highest E_{mod} that can be applied. Hence one would more likely need $V \leq 100$ V and several centimeters long modulators for π-phase modulation. According to (6), one would deduce that the thinner the waveguide is, the smaller would be the voltage (or the length) needed for π-phase shift.

A perturbation analysis has been carried out at Washington University of phase modulation of the TE_m mode in the configuration shown in Fig. 7 [23]. The result gives

$$\Delta\phi = C_{mm} V l \tag{7}$$

$$C_{mm} = \frac{k_0^2 n_f^4 r_{41}}{2\beta_m d} \left[\frac{\beta_m}{2\omega\mu_0} \int_0^d E_m(x) E_m^*(x)\, dx \right] \tag{8}$$

$$V_\pi = \pi / C_{mm} l. \tag{9}$$

Here β_m is the propagation wavenumber of the TE_m mode; E_m is the transverse electric-field variation of TE_m mode given in [14], and [15]; the quantity in the bracket is the normalized overlap integral expressing the percentage of the power of the TE_m mode being transmitted inside the film. The overlap integral is present because there is no Δn in the regions of the evanescent tails of the TE_m mode. When the film is thick, the overlap integral

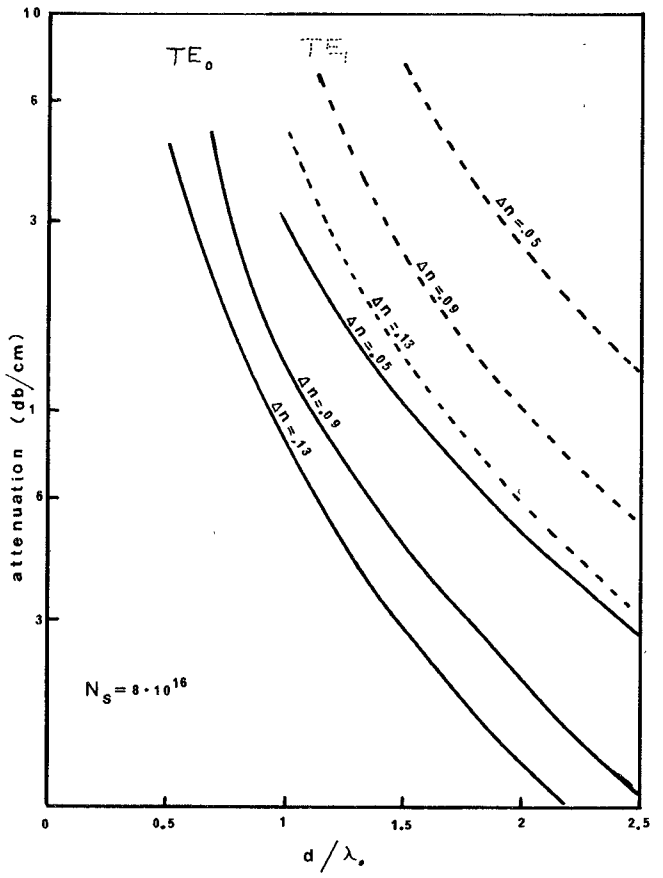

Fig. 6. Attenuation rate of GaAs/GaAsP waveguides.

is approximately one and $\beta_m \cong k_0 n_f$; (7) is identical to (5). But, if one wishes to optimize the modulator performance, (8) predicts that there is an optimum d value that will yield the largest C_{mm} coefficient. When d is too small (i.e., very near the cutoff of the TE_m mode), $\Delta\phi$ is smaller again because the decrease in the overlap integral will more than offset the advantage obtained through the decrease in the value of d.

B. Electrooptical Amplitude Modulation by Diffraction

In thin-film waveguides, it is difficult to excite both the TE and the TM modes efficiently at the same time for polarization modulation. Therefore, Bragg diffraction or mode conversion are used to achieved amplitude modulation [24]–[26]. A Bragg-diffraction modulation has been fabricated on the GaAs/n^+GaAs waveguide as illustrated in Fig. 8 [27]. In this modulator, some of the Schottky-barrier grating fingers have low breakdown voltage because of the random defects under a few electrodes. Hence individual fingers were tested and only the "good" Schottky-barier fingers were interconnected on top of the SiO_2 insulating pad to give the modulation field. Approximately 1 percent of the amplitude modulation was obtained when 60 V were applied.

It is well known that the behavior of such a modulator can be analyzed by coupled-mode analysis [28], [29]. An analysis performed for the Bragg modulator in GaAs waveguides gives the following results [23]

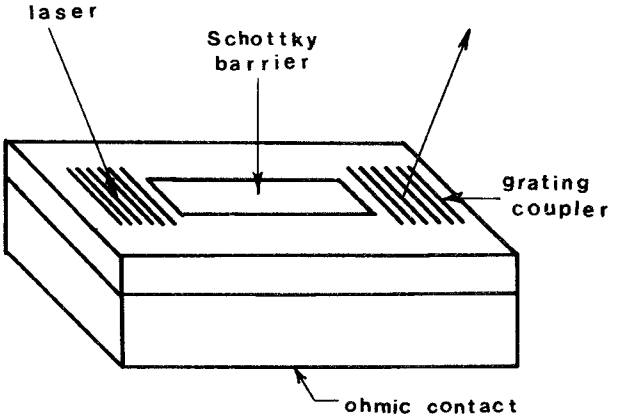

Fig. 7. Illustration of an experiment on electrooptical phase modulation (from [17] and [23]).

$$R = \exp(-\alpha l)\cos[\pi^{-1}\cos\psi\, C_{mm} V l]$$
$$S = \exp(-\alpha l)\sin[\pi^{-1}\cos\psi C_{mm} V l] \qquad (10)$$

where R is the amplitude of the incident TE_m mode; S is the amplitude of the diffracted TE_m mode; ψ is the angle of diffraction between the incident direction and the diffractured direction

$$\beta_m \sin\psi = 2\pi/L$$

when L is the periodicity of the electrode pattern. From (10), it is clear that 100-percent amplitude is obtained when

$$V = \frac{\pi^2}{2\cos\psi C_{mm} l} = V_{100}. \qquad (11)$$

Hence, we expect that V_{100} will be larger than V_π by the factor of $\pi/2\cos\psi$. Note that optimization of both of the phase modulation and Bragg's diffraction modulation will occur at the same waveguide thickness.

Amplitude modulation could also be obtained by mode conversion when the grating grooves are perpendicular to the direction of propagation of the TE_m mode [28]–[30].

The forward mode-conversion process is inefficient because of the small overlap integral value [26]. The backward mode-conversion process is difficult to achieve experimentally because this process requires small L values. When the L value is smaller than the epitaxial film thickness d, the periodic pattern of Δn is also degraded. For these two reasons, Bragg diffraction is more preferable for electrooptical modulation.

C. Electrooptical Amplitude Modulation by Beam Steering

Cheo reported that if a guided wave is propagated along the edge of a Schottky-barrier electrode (i.e., with part of the beam under the electrode and part of the beam outside of the electrode), then the phase shift caused by the electrooptical effect on one-half of the beam will interfere with the other half of the unperturbed beam so that the direction of propagation of the total beam is shifted [31]. Let the electrooptical phase shift for one-half of the beam be $\Delta\phi$. The shift in the angular direction of

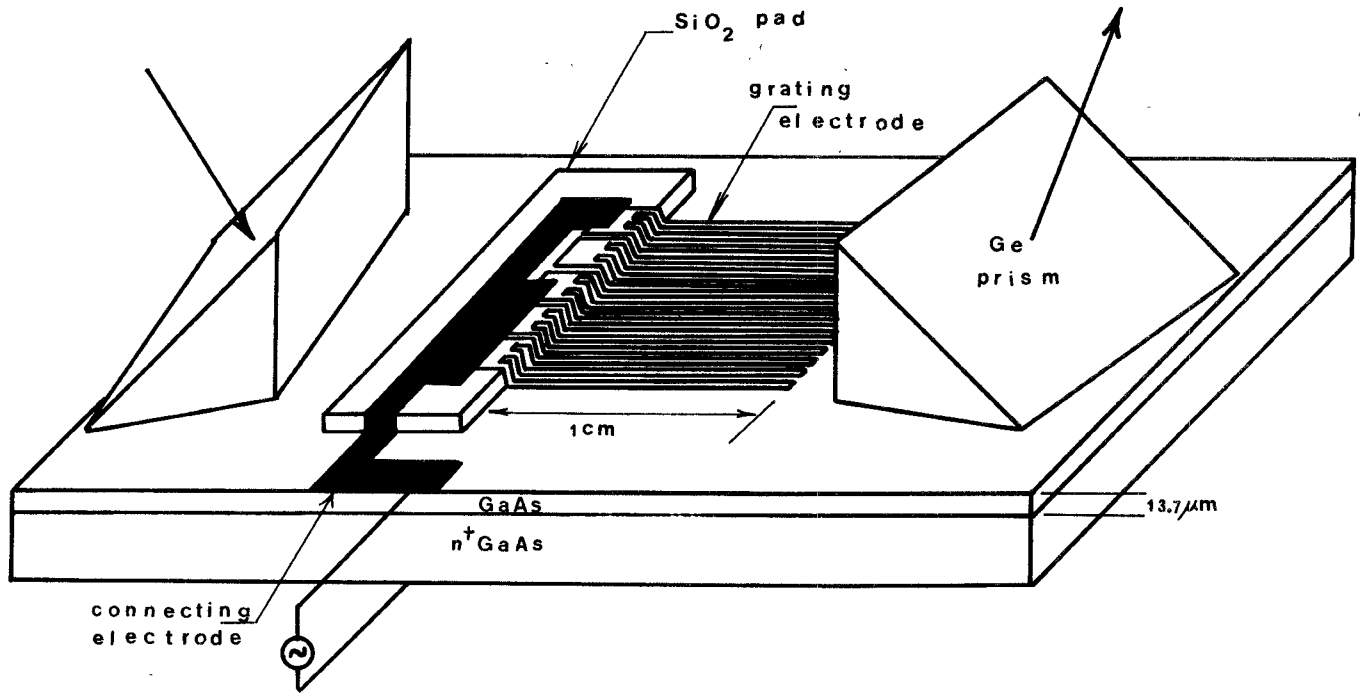

Fig. 8. Illustrations of electrooptical modulation by Bragg diffraction.

the beam caused by $\Delta\phi$ is

$$\Delta\psi = \Delta\phi/k_0 W \tag{12}$$

where W is the total width of the guided-wave beam. 10^{-3} rad of $\Delta\psi$ was obtained experimentally with l = 0.5 cm, V = 50 V, W = 0.3 mm, and d = 20 μm in GaAs/n^+GaAs waveguide. This amount of $\Delta\psi$ yielded 12.8-percent amplitude modulation. In order to get a $\Delta\psi$ large enough to resolve the shifted beam from the original beam, one needs

$$\Delta\psi \geq \lambda/2W \quad \text{or} \quad \Delta\phi \geq \pi. \tag{13}$$

In other words, the condition for fully resolving the shifted beam is equivalent to the condition for obtaining π-phase shift in phase modulation.

D. Figure of Merits and Comparison of Electrooptical Modulation Processes

V_π and V_{100} are only one of the figures of merit that can be used to measure the effectiveness of the modulation process. From the driver's point of view, the modulator is nothing but a capacitor C in parallel with an internal spread resistance R_{int}. It is well known that the second figure of merit to be considered is the required modulation power per unit bandwidth $P/\Delta f$ for achieving π-phase shift or 100-percent amplitude modulation [32]. For the thin-film modulators discussed here [23]

$$P/\Delta f = \frac{\epsilon_r}{72}\left(\frac{\lambda}{n_f^3 r_{41}}\right)^2\left(\frac{\beta_m}{n_f k_0}\right)^2\left(\frac{W}{l}\right) \cdot\left[d \Big/ \left(\frac{\beta_m}{2\omega\mu_0}\int_0^d E_m(x)E_m^*(x)\,dx\right)\right] \tag{14}$$

for phase modulation (in case of beam-steering modulation, replace W/l by $W/2l$), and for Bragg modulation

$$P/\Delta f = \frac{\epsilon_r}{72}\frac{\pi^2}{8\cos^2\psi}\left(\frac{\lambda}{n_f^3 r_{41}}\right)^2\left(\frac{\beta_m}{n_f k_0}\right)^2\left(\frac{W}{l}\right) \cdot\left[d \Big/ \left(\frac{\beta_m}{2\omega\mu_0}\int E_m E_m^*\,dx\right)\right]. \tag{15}$$

It is clear now that at frequencies below 1 GHz, when RF power dissipation in the substrate is not an important consideration, electrooptical modulation can be optimized in epitaxial thin-film waveguides using the transverse electrode configuration by a) finding the thickness d that will maximize the C_{mm}; b) using a minimum W/l ratio that is allowed by the diffraction-limited beam spread; and c) choosing a waveguide structure that will have low attenuation. Condition c) can be met by either the GaAs/GaAsP or the GaAs/GaAlAs waveguide. GaAs/n^+GaAs waveguides are at a disadvantage because they will have a high attenuation rate when d is less than 15 μm. To reduce the effect of absorption from the metallic electrode, a buffer layer with refractive index lower than the index of the film will be deposited or grown on top of the guiding film [23]. To reduce RF power dissipation in the waveguide structure, reverse-biased Schottky-barrier electrode, or high-resistivity film ($\rho > 10^5$ Ω·cm), or reverse-biased p-n junction coincident with the waveguiding layer must be used to limit the current passing through the modulator.

Fig. 9 shows the calculated curve of C_{mm} versus the film thickness d in GaAs epitaxial waveguide for Δn = 0.11 and Δn = 0.05. These Δn's can be obtained experimentally fairly easily in GaAs/GaAs$_{1-x}$P$_x$ and in GaAs/

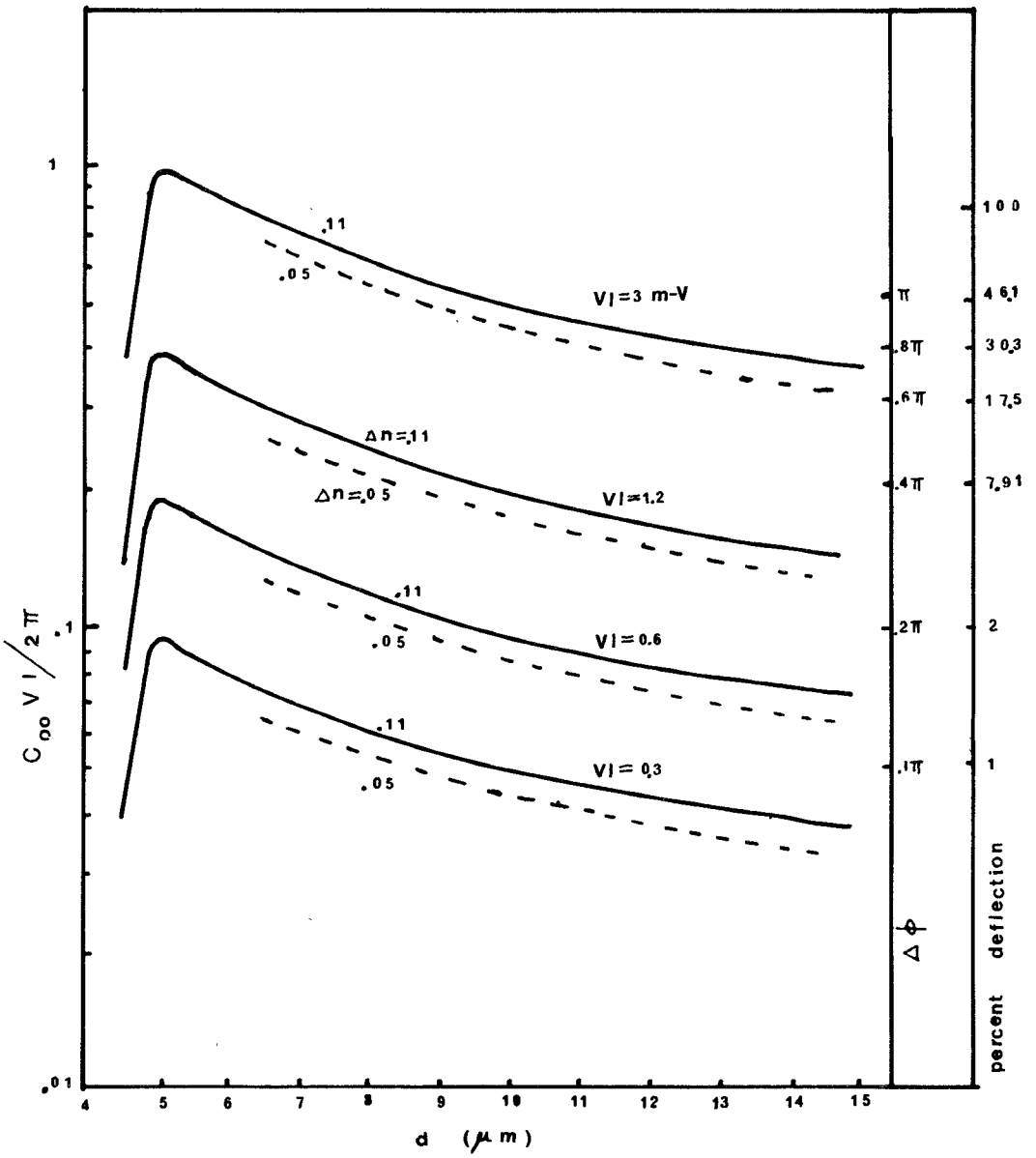

Fig. 9. Efficiency of electrooptical modulation in GaAs epitaxial thin-film waveguides.

$Ga_{1-y}Al_yAs$ waveguides with $x \cong y = 0.28$ and $x = y \cong 0.14$. The correspondent $\Delta\phi$ and the fraction of the guided-wave power in the diffracted beam obtained in the Bragg's diffraction for $\psi \simeq 0$ are given as the vertical scale shown on the right-hand side of the same figures. Here the scales are nonlinear and are made to fit the functional relationship expressed in (7) and (10). Note that when $C_{mm}lV/\pi$ is larger than $\pi/2$, the diffraction efficiency will again be less than 100 percent. In Fig. 10 we have plotted the curves of $P/\Delta f$ versus d for the same waveguides with $\Delta n = 0.11$.

Note that there is a minimum W/l ratio that can be used, restricted by the minimum beam divergence from a given aperture. It has been shown in the bulk modulator that the minimum W/l ratio is [32]

$$\frac{W^2}{l} = (S^2)\frac{8}{\beta_m}$$

where S is the safety factor. Applying that minimum ratio to the guided-wave modulators we see that for $S = 2$

$$(W/l)_{\min} = 4 \times 10^{-2}, \quad \text{for } l = 1 \text{ cm}$$

$$(W/l)_{\min} = 1.8 \times 10^{-2}, \quad \text{for } l = 5 \text{ cm}.$$

Thus the best calculated $P/\Delta f$ that one can get for guided electrooptical modulation in $GaAs/GaAs_{0.72}P_{0.28}$ or in $GaAs/Ga_{0.72}Al_{0.28}As$ waveguides is approximately 1.5 W/MHz with $l = 5$ cm and $d \cong 5$ μm.

Alternatively, parallel interdigital-electrode configuration can be used [24], [25] to avoid the use of a low-resistivity substrate. Although no experimental data are available for this configuration at the 10.6-μm wavelength, one would expect that V_π and V_{100} will be larger and that the capacitance will be lower than the voltages and capacitances for the transverse-electrode configuration.

II–VI semiconductors such as CdTe have a larger electrooptical effect than GaAs. But no electrooptical modulation has been reported today in those waveguides.

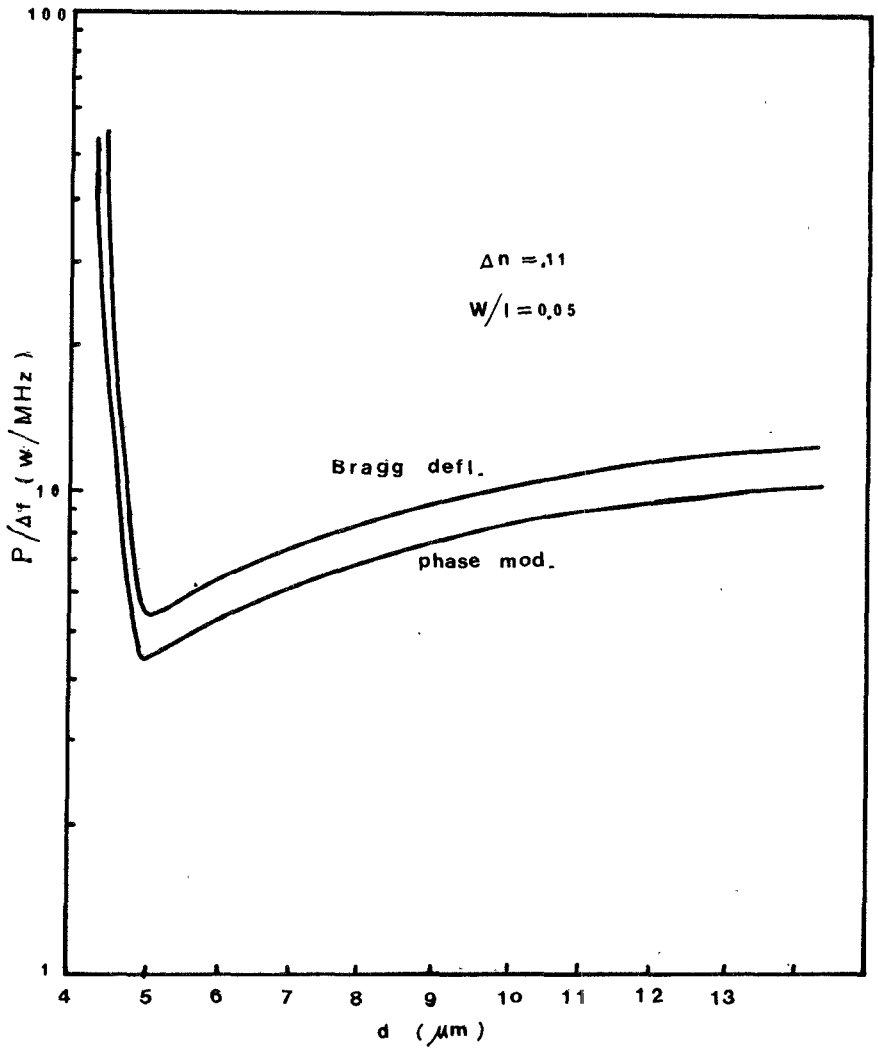

Fig. 10. Modulation power per unit bandwidth required for electrooptical modulation in GaAs epitaxial thin-film waveguides.

As in the case of bulk modulators, amplitude modulation is expected to be nonlinear due to the sinusoidal dependence on the applied voltage [23], [32].

E. Electrooptical Modulation in Two-Dimensional Waveguides

Electrooptical modulation in uniform thin-film wave is much superior than in the case of bulk modulators [21], [23], [31], [33], [34]. But it has low RF impedence and still requires hundreds of watts of power to drive it. The low impedence and the large $P/\Delta f$ value are caused primarily by the large capacitance produced by the large electrode areas across a film a few microns thick. The capactitance could be reduced significantly if two-dimensional waveguides (described in Section II-D) were used. Fig. 11 demonstrates the calculated phase shifts and the power per unit bandwidth obtainable in a two-dimensional phase modulator [23]. It was shown analytically [23] that amplitude modulation in a two-dimensional modulator can also be obtained if a two-dimensional electrode pattern is used to phase match the $E_{pq}{}^{y}$ mode to the $E_{pq'}{}^{y}$ mode as shown in Fig. 12. In Fig. 11 l is chosen to be 5 cm or less in view of the sample size that can be obtained in practice; W is chosen to be 50 μm so that a reasonable amount of the CO_2-laser power can be transmitted.

F. Microwave Electrooptical Modulation

Ultimately, the bandwidth of any electrical lumped-element modulator described in Sections II-A–C will be limited by the transit time that it will take the guided wave to propagate across the entire length of the modulator [32]. For $l = 5$ cm, the transit time will limit the modulation bandwidth to less than 1 GHz. For modulation frequencies above this limit, traveling-wave modulators must be considered. In that case, matching of both the phase and the group velocities of the optical and the modulating waves must be obtained [26], [32].

At frequencies higher than the UHF–VHF range, RF power dissipation in the low-resistivity substrate layer also becomes a problem. In order to achieve electrooptical modulation at 10 GHz, Cheo and Gilden at the United Aircraft Research Laboratory have chosen to polish a piece of 3-cm-long high-resistivity GaAs down to 20 μm thick (without any low-resistivity material surrounding

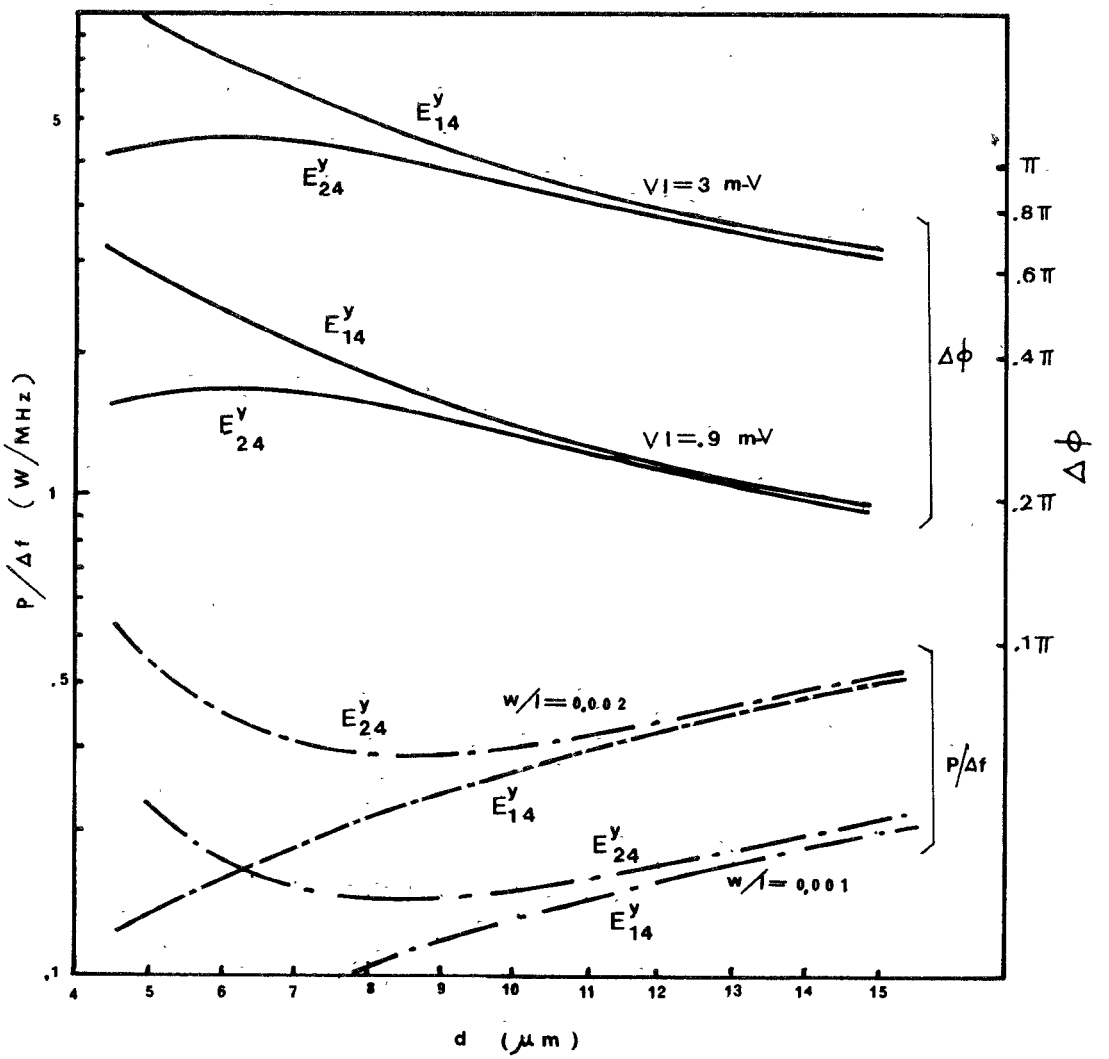

Fig. 11. Characteristics of electrooptical phase modulation in two-dimensional GaAs/$GaAs_{0.72}P_{0.28}$ waveguides.

it) as their waveguide [33]. This thin-film waveguide is then placed inside a minigap microwave ridge waveguide. The interaction between optical guided wave and the synchronous traveling microwave produced a phase shift in the guided-wave mode. Broad coupling of the microwave into the thin film were obtained.

G. Modulation by Carrier Injection

Experimental observation of beam steering as well as absorption of the guided wave in GaAs/GaAlAs waveguides by carrier injection has been reported by McFee *et al.* [13], [35]. In the case of optical injection, a pulsed UV N_2 laser was used to irradiate a strip-shaped area ($\cong 5 \times 0.1$ mm) of GaAs waveguide surface with peak density $\approx 5 \times 10^5$ W/cm^3 as shown in Fig. 13. It was estimated that 5×10^{18} electrons per cubic centimeter were injected about 1 μm deep at the surface of the GaAs waveguide. From (1) and (4), it is clear that the injected carrier would create an enormous absorption coefficient of 400 cm^{-1} and a change of refractive index of 1.54. Experimentally, they observed that the full power of an N_2 laser is more than sufficient to completely attenuate the guided wave. When pump power is reduced the dominant effect is to deflect the guided wave in the plan of the film. Deflections of order of 1°–2° have been observed.

For electrical injection of carriers, a p-type GaAlAs mesa is grown on the GaAs waveguiding layer. Substantial amplitude modulation of the guided wave results when a positive voltage pulse is applied, creating a current density of approximately 100 A/cm^2. Long decay time of the order of hundreds of nanoseconds were observed when the carriers are injected electrically as compared to tens of nanoseconds decay time in optical injection.

H. Modulation by Surface Acoustic Waves

Surface acoustic waves could also be used to provide both periodic variations of Δn and surface corrugations [36]–[38]. Although switching and modulation of an optical guided wave by surface acoustic waves have been quite successful in the visible-light wavelength [36]–[38], the extension of this technique to the far infrared has not been as successful. The primary difficulties are that the efficiency bandwidth product of acoustooptical modulation

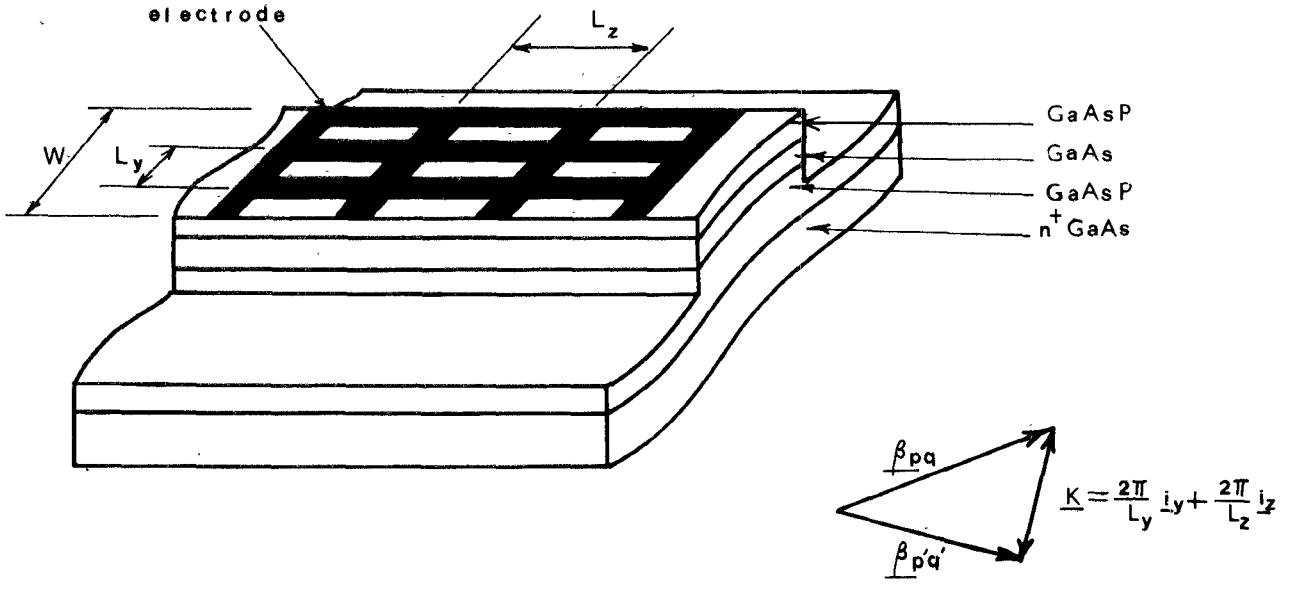

Fig. 12. Illustration of a proposed amplitude modulator in two-dimensional GaAs/GaAsP waveguides.

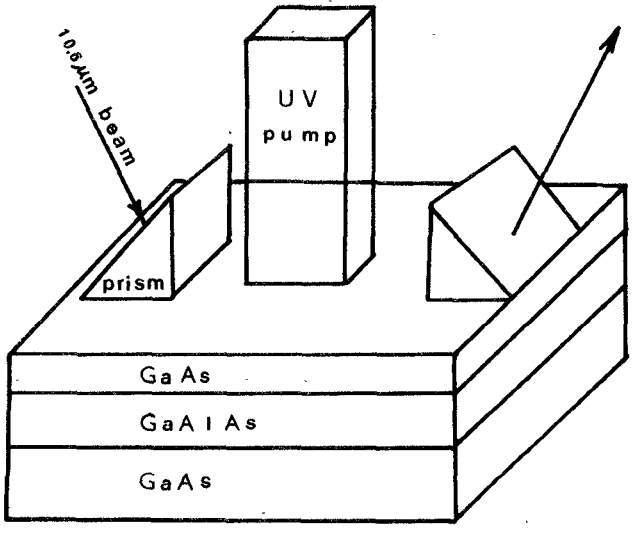

Fig. 13. Illustration of modulation by carrier injection (from [28]).

is proportional inversely to the wavelength cubed. In view of both the limited acoustic power available from the transducers and the long transit time for the acoustic wave to reach a steady state across the width of the laser beam, acoustooptical modulation does not appear to be attractive for 10.6-μm wavelength applications [39].

IV. PASSIVE WAVEGUIDE COMPONENTS

A. Input–Output Coupling

Both the prism and the grating couplers have been used successfully at 10.6-μm wavelength to couple in and out of thin-film waveguides [9], [11]–[13]. However, because of the high refractive index of GaAs, excitation efficiency is usually quite small ($\sim$10 percent) for forward excitation from the air region using a shallow grating coupler [11], [40]. Using the backward excitation, an efficiency of 30 percent was achieved [33]. Ultimately, if a deep grating or a substrate mode is used for backward excitation, higher grating excitation efficiency may be obtained [40], [41]. Coupling efficiency in the order of 30–50 percent should be able to be achieved routinely with prisms without any special effort. In order for prisms to have a higher refractive index than the film, Ge is used. Gratings can usually be etched either chemically or by sputtering from masks produced by conventional photolithography.

B. Mode Conversion and Directional Coupling

Beam splitting, directional coupling, and mode conversion could also be achieved via periodic Δn produced by etching of the waveguide surface [14], [28], [29], [42]. In principle, by controlling the grating depth and the interaction length, one should be able to obtain any amount of direction coupling or mode conversion, from 0 to 100 percent. However, in practice, because there are radiation losses created by etching and because there are the nonuniformities in the film thickness and in the etched-groove depth, it is difficult to predict the exact behavior of the fabricated devices. A mode converter has been fabricated by Sopori [42]. Here, an etched grating is used to divert a desired amount of power from the incident guided-wave mode to the scattered guided-wave mode. Fig. 14 shows the calculated results of the ratio of the power in the scattered beam to the power in the incident beam as a function of the groove depth. The solid curve represents the case where the incident beam is a TE_0 mode; the dashed curve represents the case where the incident beam is a TE_1 mode. The experimental points are marked by the vertical bars, where the height of the bar represents the estimated error in the experimental measurements. The discrepancy between experimental data and theoretical calculation demonstrates the difficulty in controlling all the necessary parameters in the fabrication of such a device.

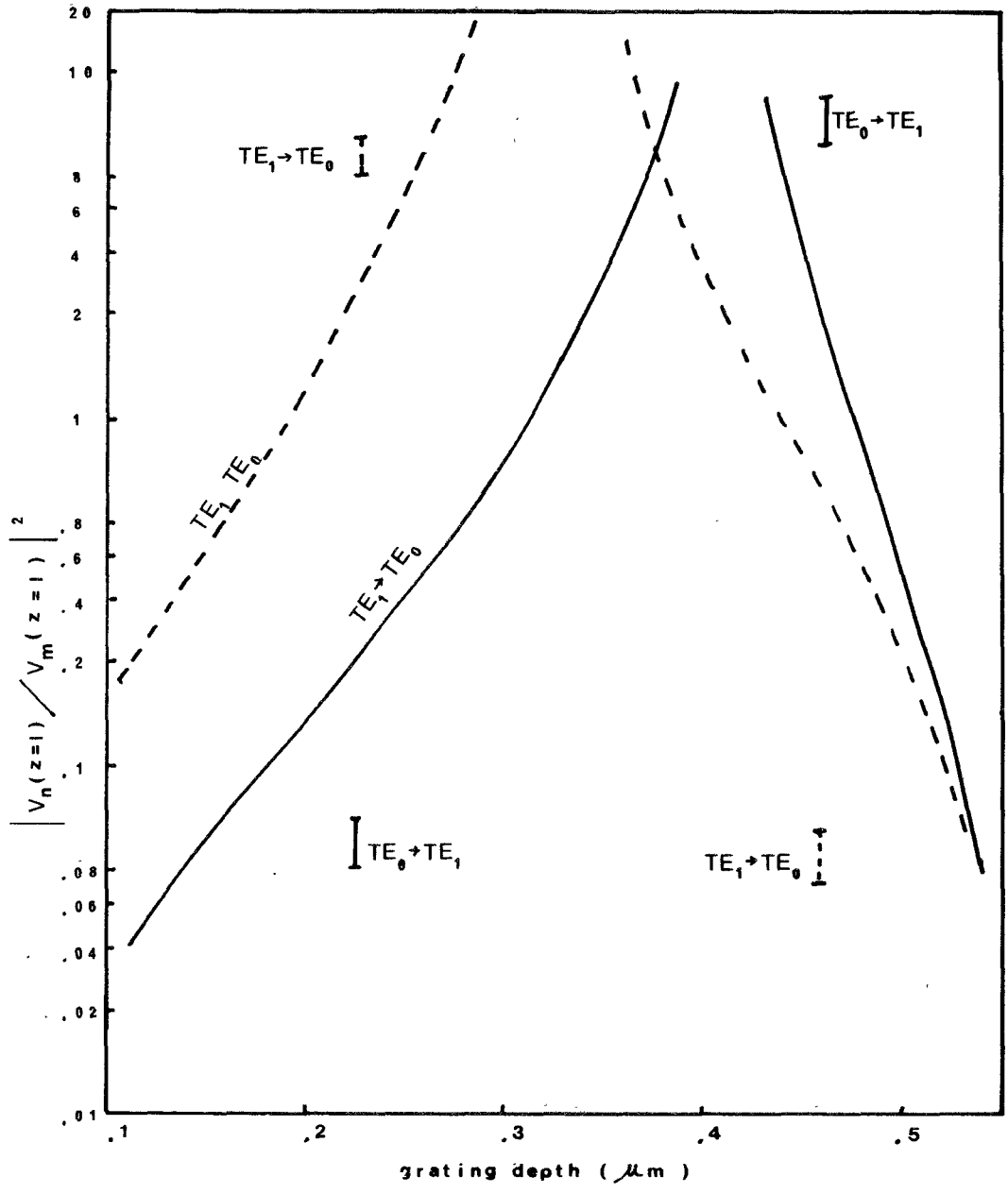

Fig. 14. Characteristics of an etched-grating mode converter in GaAs/n$^+$GaAs thin-film waveguides.

V. WAVEGUIDE LASERS

The use of hollow dielectric waveguides both to guide the laser radiation and to confine a gas discharge was proposed by Marcatilli and Schmeltzer [43]. Subsequently, CO_2 waveguide lasers were reported by various researchers [1], [2], [44], [45]. Although the hollow-dielectric-tube CO_2 waveguide laser is not in a thin-film configuration that can be integrated easily with thin-film waveguide components, its characteristics are superior to the conventional CO_2 laser in certain aspects for low-power communication applications. Here again we see that guided-wave technology is used to improve the performance of an individual device.

Typically, laser oscillation was achieved in a capillary tube with conventional external reflectors that match the fundamental free-space Gaussian beam to the entrance of the capillary tube. Both the flowing gas and the sealed-tube design have been investigated. Typically, the tube is filled with a mixture of CO_2, N_2, and He gas. In such a small-bore tube, favorable deexcitations by wall collisions and reduction of gas temperature because of the improved thermal conduction of the wall were obtained. CO_2-laser operation can be obtained at gas pressures in excess of 300 torr. Consequently, increased gains, much broader linewidth, and more power generated per unit volume were observed. The latest published data indicate that power per unit length of the tube of the order of a fraction of a watt per centimeter and a tunable bandwidth on the order of hundreds of megahertz can be obtained in these lasers. Better performance at higher gas pressures is expected from researches currently being conducted at Hughes, NASA, United Aircraft, and Lincoln Laboratories.

CO_2 waveguide lasers offer attractive possibilities for compact single-mode laser oscillators and high-gain laser amplifiers. In addition, the large bandwidth obtained through the high pressure will allow us to obtain much higher intercavity modulation bandwidth [3]–[5] or larger tuning range [1], [2].

VI. CONCLUSIONS

Guided-wave technology has been used successfully to improve the performance of a number of individual components, especially that of the modulators and the lasers. Demonstration of integrated optical concepts such as two-dimensional waveguides, mode conversion via etched grating, etc., can easily be performed at the long infrared wavelength. However, optical communication sybsystems, combining several guided-wave components together, have not yet been developed. It is doubtful that guided-wave technology at the 10.6-μm wavelength will be used fully in the visible-light integrated-optics fashion unless an effective fiber can be developed in the future.

The most significant advance to date is the initial demonstration of efficient modulation that can be achieved by the guided-wave technique. The actual modulators that will be used in communication systems will be slightly different to the ones reported in the literature. For example, buffer film will be used on top of the GaAs film to reduce the insertion loss caused by metallic absorption. One may want to have less than 100-percent amplitude or π-phase modulation in order to reduce either the drive power or the nonlinearity of the modulated signal.

REFERENCES

[1] J. J. Degnan, H. E. Walker, J. H. McElroy, and N. McAvoy, "Gain and saturation intensity measurements in a waveguide CO_2 laser," *IEEE J. Quantum Electron.* (Corresp.), vol. QE-9, pp. 489–491, Apr. 1973.

[2] R. L. Abrams and W. B. Bridges, "Characteristics of sealed-off waveguide CO_2 lasers," *IEEE J. Quantum Electron.*, vol. QE-9, pp. 940–946, Sept. 1973.

[3] A. L. Scholtz and G. Schiffner, "CO_2-laser traveling-wave intracavity GaAs coupling modulator for nanosecond pulses," *IEEE J. Quantum Electron.* (Corresp.), vol. QE-10, pp. 457–459, Apr. 1974.

[4] N. McAvoy, J. Osmundson, and G. Schiffner, "Broadband CO_2 laser coupling modulation," *Appl. Opt.*, vol. 11, pp. 473–474, 1972.

[5] J. E. Kiefer, T. A. Nussmeier, and F. E. Goodwin, "Intracavity CdTe modulators for CO_2 lasers," *IEEE J. Quantum Electron. (Part II of Two Parts: Special Issue on 1971 IEEE/OSA Conference on Laser Engineering and Applications)*, vol. QE-8, pp. 173–179, Feb. 1972.

[6] I. Melngailis, M.I.T. Lincoln Laboratory, Lexington, Mass., private communication.

[7] W. L. Wolfe, *Handbook of Military Infrared, Office of Naval* Research, Washington, D. C., 1965 (published by the Superintendent of Documents, U. S. Government Printing Office, Washington, D. C. 20402).

[8] S. S. Ballard, K. A. McCarthy, and W. L. Wolfe, "Optical material for infra-red instrumentation," IRIA Rep. 2389-11-S, 1959 (*Supplement 2389-11-S*, Ann Arbor, Mich.: Univ. of Michigan Press, 1961).

[9] W. S. C. Chang and K. W. Loh, "Experimental observation of 10.6 μm guided waves in Ge thin films," *Appl. Opt.*, vol. 10, pp. 2361–2362, 1971.

[10] D. Hall, A. Yariv, and E. Garmire, "Observation of propagation cutoff and its control in thin optical waveguides," *Appl. Phys. Lett.*, vol. 17, pp. 127–129, 1970.

[11] P. K. Cheo, J. M. Berak, W. Oshinsky, and J. L. Swindal, "Optical waveguide structures for CO_2 lasers," *Appl. Opt.*, vol. 12, pp. 500–509, 1973.

[12] D. Finn, W. O. Groves, L. G. Hellwig, M. G. Craford, W. S. C. Chang, M. S. Chang, and B. L. Sopori, "Low-loss large area GaAs/GaAsP heterostructure as optical waveguides at 10.6 μm," *Opt. Commun.*, vol. 11, pp. 201–203, 1974.

[13] J. H. McFee, M. A. Pollack, W. W. Rigrod, and R. A. Logan, "Heterostructure GaAs-GaAlAs planar waveguides for 10.6 μm," in *Digest Tech. Papers, IEEE/OSA Topical Meet. Integrated Optics* (New Orleans, La.), Jan. 21–24, 1974, pp. MA7-1–MA7-4.

[14] D. Marcuse, *Light Transmission Optics.* New York: Van Nostrand-Reinhold, 1972.

[15] P. K. Tien, "Light waves in thin films and integrated optics," *Appl. Opt.*, vol. 10, pp. 2395–2413, 1971.

[16] S. Kamath, "Epitaxial GaAs-(GaAl)As layers for integrated optics," in *Digest Tech. Papers, IEEE/OSA Topical Meet. Integrated Optics* (New Orleans, La.), Jan. 21–24, 1974, pp. TuA10-1–TuA10-3.

[17] R. Weil, "Interference of 10.6μ coherent radiation in a 5 cm long gallium arsenide parallelepiped," *J. Appl. Phys.*, vol. 40, pp. 2857–2859, 1969.

[18] W. E. Martin and D. B. Hall, "Optical waveguide by diffusion in II-VI compounds," *Appl. Phys. Lett.*, vol. 21, pp. 325–327, 1972.

[19] W. H. Weber and K. F. Yeung, "Waveguide and luminescent properties of thin film Pb-salt injection lasers," *J. Appl. Phys.*, vol. 44, pp. 4991–5000, 1973.

[20] D. L. Spears, A. J. Strauss, I. Melngailis, and J. L. Ryan, "Low-loss waveguides at 10.6 μm produced by high-energy proton bombardment of CdTe," in *Digest Tech. Papers, IEEE/OSA Topical Meet. Integrated Optics* (New Orleans, La.), Jan. 21–24, 1974, pp. ThA10-1–ThA10-4.

[21] B. L. Sopori, W. S. C. Chang, and R. Vann, "Low-loss two-dimensional GaAs epitaxial waveguides at 10.6-μm wavelength," *IEEE Trans. Microwave Theory Tech.* (Lett.), vol. MTT-22, pp. 754–755, July 1974.

[22] P. K. Cheo, "Electro-optical properties of reverse biased GaAs epitaxial thin films at 10.6 μm," *Appl. Phys. Lett.*, vol. 23, pp. 439–441, 1973.

[23] T. Ko, "An investigation of electro-optical modulation methods in GaAs epitaxial thin film waveguides at 10.6 μm wavelength," D.Sc. dissertation, Dep. Elec. Eng., Washington Univ., St. Louis, Mo., 1974.

[24] J. H. Hammer, D. J. Channin, and M. T. Duffy, "Fast electro-optic waveguide deflector modulator," *Appl. Phys. Lett.*, vol. 23, pp. 176–177, 1973.

[25] J. N. Polky and J. H. Harris, "Interdigital electro-optic thin film modulator," *Appl. Phys. Lett.*, vol. 21, pp. 307–309, 1972.

[26] W. S. C. Chang, M. W. Muller, and F. J. Rosenbaum, "Integrated optics," in *Laser Applications*, vol. II, M. Ross, Ed. New York: Academic, 1974, pp. 227–343.

[27] W. S. C. Chang, T. Ko, B. Sopori, M. G. Craford, and D. Finn, "Electro-optic modulation at 10.6 μm in epitaxial GaAs waveguides," in *Digest Tech Papers, IEEE/OSA Topical Meet. Integrated Optics* (New Orleans, La.), Jan. 21–24, 1974, pp. WA3-1–WA3-2.

[28] A. Yariv, "Coupled-mode theory for guided-wave optics," *IEEE J. Quantum Electron.*, vol. QE-9, pp. 919–933, Sept. 1973.

[29] D. Marcuse, *Theory of Dielectric Optical Waveguides.* New York: Academic, 1974.

[30] L. Kuhn, P. F. Heidrich, and E. G. Lean, "Optical guided wave mode conversion by an acoustic surface wave," *Appl. Phys. Lett.*, vol. 19, pp. 428–430, 1971.

[31] P. K. Cheo, "Pulse amplitude modulation of a CO_2 laser in an electro-optic thin film waveguide," *Appl. Phys. Lett.*, vol. 22, pp. 241–244, 1973.

[32] F. S. Chen, "Modulators for optical communications," *Proc. IEEE (Special Issue on Optical Communication)*, vol. 58, pp. 1440–1456, Oct. 1970.

[33] P. K. Cheo and M. Gilden, "Microwave modulation of CO_2 lasers in GaAs optical waveguides," *Appl. Lett.*, vol. 25, pp. 272–274, 1974.

[34] W. B. Gandrud, "Reduced modulator drive-power requirements for 10.6-μ guided waves," *IEEE J. Quantum Electron.*, vol. QE-7, pp. 580–581, Dec. 1971.

[35] J. H. McFee, R. E. Nahory, M. A. Pollack, and R. A. Logan, "Beam deflection and amplitude modulation of 10.6 m guided waves by free carrier injection in GaAs-AlGaAs heterostructures," *Appl. Phys. Lett.*, vol. 23, pp. 571–573, 1973.

[36] L. Kuhn, M. L. Dakss, P. F. Heidrich, and B. A. Scott, "Deflection of an optical guided wave by a surface acoustic wave," *Appl. Phys. Lett.*, vol. 17, pp. 265–267, 1970.

[37] J. F. Weller, T. G. Giallorenzi, and A. F. Milton, "Light deflection in single and multimode waveguides using the acousto-optic interaction," in *Digest Tech. Papers, IEEE/OSA Topical Meet. Integrated Optics* (New Orleans, La.), Jan. 21–24, 1974, pp. WA9-1–WA9-3.

[38] R. V. Schmidt, I. P. Kaminow, and J. R. Carruthers, "Acousto-

optic diffraction of guided optical waves in $LiNbO_3$," *Appl. Phys. Lett.*, vol. 23, pp. 417–419, 1973.
[39] P. K. Cheo, United Aircraft Research Laboratories, East Hartford, Conn., private communications.
[40] K. Ogawa, W. S. C. Chang, B. L. Sopori, and F. J. Rosenbaum, "A theoretical analysis of etched grating couplers for integrated optics," *IEEE J. Quantum Electron. (Part I of Two Parts)*, vol. QE-9, pp. 29–42, Jan. 1973.
[41] D. G. Dalgoutte, "A high efficiency thin grating coupler for integrated optics," *Opt. Commun.*, vol. 8, pp. 124–127, 1973.
[42] W. S. C. Chang, "Periodic structures and their applications in integrated optics," *IEEE Trans. Microwave Theory Tech. (1973 Symposium Issue)*, vol. MTT-21, pp. 775–785, Dec. 1973.
[43] E. A. J. Marcatillis and R. A. Schmeltzer, "Hollow metallic dielectric waveguides for long distance optical transmission and lasers," *Bell Syst. Tech. J.*, vol. 43, pp. 1783–1809, 1964.
[44] T. J. Bridges, E. G. Buckhardt, and P. W. Smith, "CO_2 waveguide lasers," *Appl. Phys. Lett.*, vol. 20, pp. 403–405, 1972.
[45] R. E. Jenson and M. S. Tobin, "CO_2 waveguide laser," *Appl. Phys. Lett.*, vol. 20, pp. 408–510, 1972.

GaAs and GaAlAs Devices for Integrated Optics

VIKTOR EVTUHOV, MEMBER, IEEE, AND AMNON YARIV, FELLOW, IEEE

(Invited Paper)

***Abstract*—The emergence of a monolithic optical circuit technology depends on the availability of materials capable of performing complex electrooptic functions and on the development of new fabrication techniques. The work done on GaAs and its related alloys is reviewed and summarized, and their feasibility for integrated optical circuits is examined.**

I. INTRODUCTION AND CHRONOLOGICAL REVIEW

THE FIELD of integrated optics has as its professed goal the eventual fabrication of complex optical circuits in small solid configurations. Such circuits will become necessary if the many hopes for optical communication and optical computers are ever to come true.

The main motivation for this work derives from the spectacular success of integrated electronics where a single "mother" material—silicon—is used to fabricate extremely complex circuits.

Although the nature of optical interactions is such that we are not likely to approach the component density of integrated electronics, the inherent simplicity and reliability of single crystal circuits is reason enough to strive for optical monolithic circuits.

In this paper we will review a series of experimental and theoretical developments which took place during the period 1966–1974. These experiments have to do mostly with establishing the feasibility of performing some key optical functions in GaAs and GaAlAs crystal systems.

The interest in GaAs as a basic material for optical integrated circuits (OIC) has been stimulated by the fact that this material has a high degree of versatility in terms of its electrical and optical properties and is potentially suitable for fabrication of a variety of necessary optical circuit components. This is especially true if one considers the possibility of alloying GaAs with Al producing a ternary compound of the form $Ga_{1-x}Al_xAs$. Because the optical transmission characteristics of $Ga_{1-x}Al_xAs$ are strongly dependent on x, this material is easily tailored to allow waveguiding of various near IR wavelengths. For example, by varying x between zero and 0.3, the band edge of the compound is shifted from 9000 to 7000 Å. This will be discussed in more detail in Section II. GaAs also has high electrooptic, acoustooptic, and optical nonlinear coefficients, making it potentially applicable to a variety of switching, modulation, and frequency conversion devices. Finally, it is compatible with a number of fabrication techniques such as ion implantation, epitaxial growth, and electron beam and ion micromachining. Light-emitting diodes (LED's), lasers, modulators, switches, and detectors can be fabricated using this material. The most important properties of GaAs and $Ga_{1-x}Al_xAs$ are summarized in Table I.

GaAs and GaAlAs possess most of the properties needed to perform complex optical functions and thus hold promise for the development of monolithic optical circuits in which all the components are fabricated using basically the same material on a single chip substrate. However, the components being developed at this time in various laboratories are not tied exclusively to the monolithic circuit approach and are compatible with the "hybrid" approach where different materials are used to perform different

Manuscript received April 19, 1974. This work was supported in part by the Air Force Cambridge Research Laboratories and the Advanced Research Projects Agency and in part by the Office of Naval Research and the Army Research Office.

V. Evtuhov is with Hughes Research Laboratories, Malibu, Calif.
A. Yariv is with the Department of Electrical Engineering, California Institute of Technology, Pasadena, Calif. 91125.